Bioorganic & Medicinal Chemistry Letters xxx (xxxx) xxxx

Contents lists available at ScienceDirect

Bioorganic & Medicinal Chemistry Letters

journal homepage: www.elsevier.com/locate/bmcl

Discovery of novel heat shock protein (Hsp90) inhibitors based on luminespib with potent antitumor activity

Juyoung Jung[a,c], Jinsun Kwon[b], Soojung Hong[a], An-Na Moon[a], Jinah Jeong[a], Sungwook Kwon[a], Jeong-ah Kim[a], Myoungjae Lee[a], Hongsub Lee[a], Jin Hee Lee[a], Jeewoo Lee[c,*]

[a] Research Laboratories, Ildong Pharmaceutical Co., Hwaseong-si, Gyeonggi-do 18449, South Korea
[b] AIMS BioScience Co., 2, Baumoe-ro 27-gil, Seocho-gu, Seoul 06752, South Korea
[c] Laboratory of Medicinal Chemistry, College of Pharmacy, Seoul National University, Seoul 08826, South Korea

ARTICLE INFO

Keywords:
Heat shock protein 90
Luminespib
Antitumor agent

ABSTRACT

A series of isosteric surrogates of the 4-phenyl group in luminespib were investigated as new scaffolds of the Hsp90 inhibitor for the discovery of novel antitumor agents. Among the synthesized surrogates of isoxazole and pyrazole, compounds **4a**, **5e** and **12b** exhibited potent Hsp90 inhibition in ATPase activity and Her2 degradation assays and significant antitumor activity in A2780 and HCT116 cell lines. Animal studies indicated that compared to luminespib, their activities were superior in A2780 or NCI-H1975 tumor xenograft models. A molecular modeling study demonstrated that compound **4a** could fit nicely into the *N*-terminal ATP binding pocket.

An ATP-dependent molecular chaperone, heat shock protein 90 (Hsp90), regulates the stability and activity of client proteins that play critical roles in proliferation, survival, transformation and apoptosis.[1–4] A significant number of these client proteins, including protein kinases such as HER2, C-RAF, B-RAF, and AKT, have been implicated in oncogenesis. Simultaneous degradation of multiple oncogenic client proteins is caused by inhibition of Hsp90 in the ubiquitin-proteasome pathway.[5–8] Due to its the selectivity in inhibiting the growth of cancer cells over nontransformed cells, Hsp90 inhibition has emerged as a promising mode of action for anticancer chemotherapy.[9–10]

Geldanamycin (GD) is a natural 1,4-benzoquinone ansamycin that inhibits Hsp90 by binding to its *N*-terminal ATP-binding pocket[11] and has provided an important opportunity for understanding the role of Hsp90 in tumor growth.[12–14] Tanespimycin (17-AAG), a derivative of geldanamycin, as a single or combination drug in clinical trials, has shown broad activity and reduces drug resistance. However, 17-AAG has limited applications due to its poor solubility, bioavailability, hepatotoxicity and extensive metabolism by polymorphic enzymes.[15–17] Therefore, novel small molecule Hsp90 inhibitors have been studied to overcome this issue. Among them, resorcinol scaffolds have emerged as a new class of Hsp90 inhibitor. This class of compounds, such as luminespib (NVP-AUY922) and ganetespib (STA-9090), exhibit potent and selective Hsp90 inhibition and display significant oral activities in cellular and animal models of cancer.[18,19] In addition, purine scaffold compounds (e.g., PU-H71, BIIB021) have also been reported as Hsp90 inhibitors.[20]

In our program to discover Hsp90 inhibitors as novel antitumor agents, we investigated novel scaffolds based on luminespib in which the phenyl group was substituted with isoxazole or 2,3- or 3,4-pyrazole moieties (Fig. 1). The synthesized compounds were tested for Hsp90 inhibition by measuring their ATPase activity and ability to degrade a client protein and were evaluated for their *in vitro* cytotoxicity against cancer cell lines. The selected compounds were further evaluated for their antitumor activities in *in vivo* tumor xenograft models. The molecular modeling of representative inhibitors was performed to identify the binding mode in the *N*-terminal ATP binding pocket.

The synthesis of R_1-CH_2 substituted isoxazole derivatives (**4a–x**) is described in Scheme 1. The known iodide key intermediate **1** was prepared[18] and coupled with ethyl 5-(tributylstannyl)isoxazole-3-carboxylate[21] in the presence of tetrakis(triphenylphosphine)palladium(0) to provide the isoxazole compound **2a**. Reduction of carboxylate **2a** afforded the alcohol intermediate **3a**, which was subsequently converted into the mesylate intermediate **3e**. Alkylation of the alcohol intermediate **3a** with methylbromoacetate afforded the ethylcarbamoylether compound **3b**. Treatment of the ester **3b** with 2 *N* LiOH or 7 *N* NH_3 provided the acid **3c** or amide **3d**, respectively. Next, fluoro or cyano substitution reactions from the mesylate intermediate **3e** readily afforded the fluoromethyl **3f** and cyanomethyl **3g** isoxazoles. In addition, aminomethyl **3i** was obtained by thermal treatment of the potassium phthalimide. The others **3h–x** were obtained from the mesylate intermediate **3e** by a similar substitution reaction. Finally, removal of

* Corresponding author.
E-mail address: jeewoo@snu.ac.kr (J. Lee).

https://doi.org/10.1016/j.bmcl.2020.127165
Received 4 March 2020; Received in revised form 27 March 2020; Accepted 1 April 2020

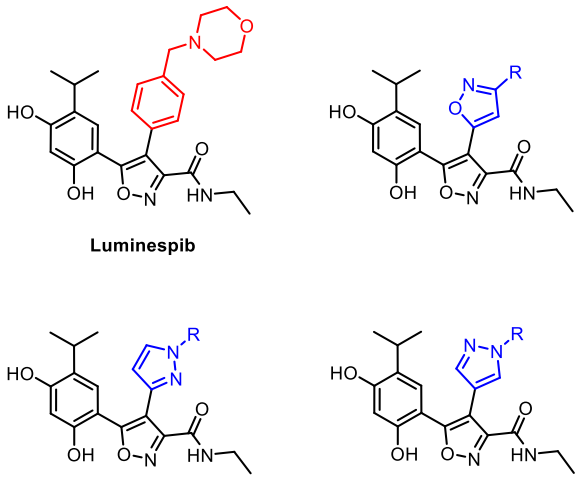

Fig. 1. Design of new scaffold Hsp90 inhibitors based on luminespib.

the dibenzyl protecting group in **3a–x** using boron trichloride provided the final compounds **4a–x**.

The synthesis of R_2-CO substituted isoxazole derivatives **5a–g** is illustrated in Scheme 2. Acid hydrolysis of the ethylcarboxylate **2a** furnished the acid **2b**. Amination of the ester **2a** with commercially available various amines afforded the requisite amide derivatives **2c–g**. Final products **5a–g** were obtained after the deprotection of the dibenzyl group.

The synthesis of 1,3-disubstituted pyrazole derivatives is shown in Scheme 3. The iodide intermediate **1** was converted into the alkyne **6** by ethnyltributyltin via the Stille reaction and as then converted into the acetyl **7**. The acetyl **7** was condensed with dimethylformamide dimethylacetal to give the dimethylaminoacryloyl **8**, which was quantitatively cyclized into the unsubstituted C3-linked pyrazole **9a** using hydrazine hydrate. Alkyl substituted pyrazoles (**9b–e**) were obtained by using appropriate alkylation reagents, followed by the deprotection of benzyl groups to produce the desired product **10a–e**.

The synthesis of 1,4-disubstituted pyrazole derivatives is presented in Scheme 4. Stille coupling of the iodide **1** with trityl pyrazole tributylstannane using Pd(0) afforded the protected C4-linked pyrazole **11a** almost quantitatively, which was deprotected to furnish C4-linked **11b**. The 1-methyl, 1-ethyl and 1-isopropyl substituted pyrazoles **11c–e** were also obtained from the iodide **1** by direct coupling with the corresponding substituted pyrazoles. The final deprotection readily provided the C4-linked pyrazoles **12b–e**.

All the synthesized compounds were tested for Hsp90 inhibition by the measurement of the ATPase activity of Hsp90 as well as by the cell-based Her2 degradation assay. For antitumor activity, their cytotoxicities were evaluated against the A2780 (human ovarian cancer) and HCT116 (human colon cancer) cell lines. The results are summarized in Tables 1–3, together with the values of luminespib (NVP) for comparison.

First, we investigated the isoxazole surrogates bearing a CH_2R^1 group (**4a–x**) at the C3 position (Table 1). The hydroxylmethyl isoxazole analogue **4a** and the O-alkyl substituted analogues **4b–d**, in which R_1 is OCH_2CO_2Me, OCH_2CO_2H, and OCH_2CONH_2, respectively, were examined. Among them, **4a** exhibited potent inhibitory activity toward Hsp90 and cancer cells, which was slightly better than that of NVP. The substitution of hydroxyl in **4a** with OMs, fluoro and cyano groups did not improve the activity. Mono- or di-substituted aminomethyl isoxazole analogues **4h–s** were also explored. Although some of the amine analogues **4j**, **4l**, **4m**, **4q**, and **4r** demonstrated promising potency, none of compounds were found to be better than NVP for inhibition of Hsp90 and tumors. Cyclicamino, such as morpholinyl, piperidinyl, pyrrolidinyl and *N*-methylpiperazinyl, analogues **4t-x** were also examined. However, this modification resulted in diminished

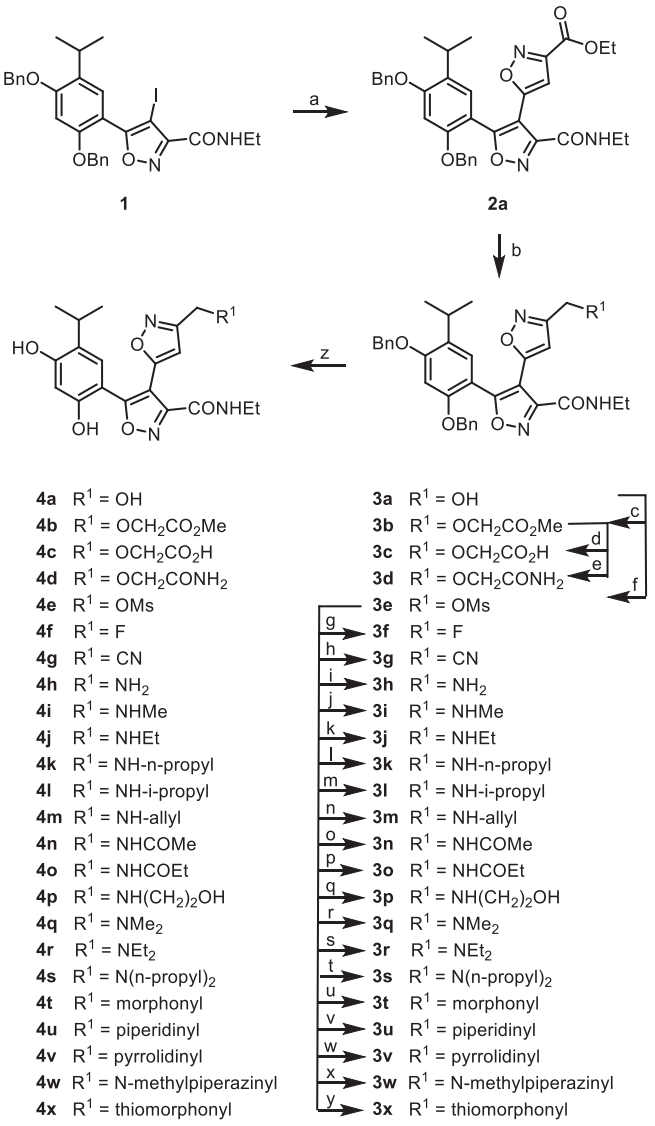

Scheme 1. Synthesis of isoxazole derivatives. *Reagents and conditions*: (a) ethyl 5-(tributylstannyl)isoxazole-3-carboxylate, $Pd(PPh_3)_4$, toluene, reflux, 2.5 h, 78%; (b) LAH, THF, 0 °C to r.t., 2 h, 61%; (c) $BrCH_2CO_2Me$, Cs_2CO_3, CH_3CN, r.t., 24 h, 61%; (d) 2 *N* LiOH, THF/water, 0 °C, 1 h, 63%; (e) 7 *N* NH_3/MeOH, KCN, 50 °C, 12 h, 89%; (f) MsCl, Et_3N, 0 °C, 3 h, 61%; (g) KF, 18-crown-6, r.t., 18 h, 78%; (h) KCN, 18-crown-6, r.t., 12 h, 98%; (i) phthalimide potassium salt, CH_3CN, reflux, 24 h, 95% and then $MeNH_2$, EtOH, reflux, 6.5 h, 99%; (j)-(y) R^1NH_2 or R^1NH, CH_2Cl_2, 8 h, 60–99%; (z) BCl_3, CH_2Cl_2, 0 °C, 0.5 h, 45–99%.

activity compared to that of the corresponding acyclic amines.

Next, we explored the isoxazole surrogates (**5a–g**) with a COR^2 group at the C3 position (Table 2). Whereas the ethyl ester **5a** and carboxylic acid **5b** showed weak activities, most amide analogues displayed reasonable inhibition toward Hsp90 and cancer cells. In particular, the ethylamide **5e** showed significantly improved activity, in which its Hsp90 inhibition and cytotoxicity in HCT116 were more potent than those of NVP.

Finally, we examined *N*-alkyl pyrazole surrogates in which the two isomers, the 1,3-pyrazole (**10a-d**) and 1,4-pyrazole (**12b-e**) analogues, were tested. Compared to NVP, most of the 1,3-pyrazole analogues have similar potencies for Hsp90 inhibition and antitumor activity. The SAR in cell-based assays clearly showed a preference for an alkyl substitution on the pyrazole moiety. The potency was enhanced when alkyl groups, such as methyl, ethyl and isopropyl, were introduced (**10b–c,**

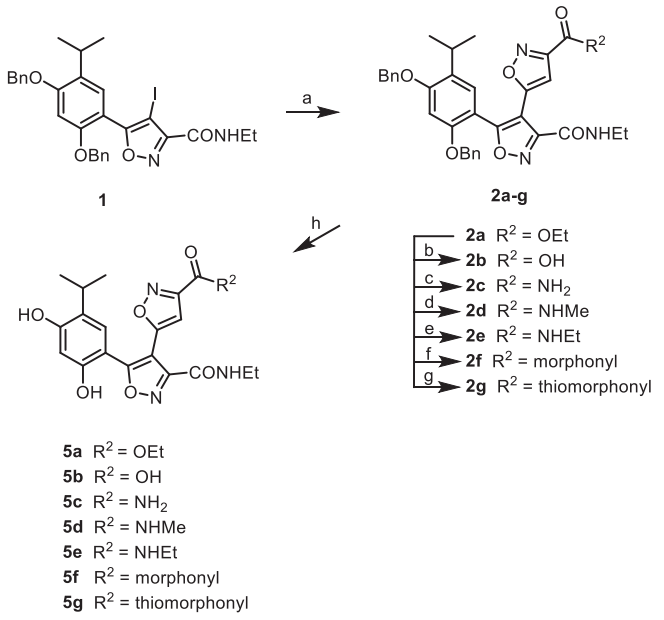

Scheme 2. Synthesis of isoxazole-3-carboxylate derivatives. *Reagents and conditions*: (a) ethyl 5-(tributylstannyl)isoxazole-3-carboxylate, $Pd(PPh_3)_4$, toluene, reflux, 2.5 h, 78%; (b) 2 *N* LiOH, THF/water, 0 °C, 1 h, 93%; (c) 7 *N* NH_3/MeOH, KCN, 50 °C, 12 h, 91%; (d) aq. 40% $MeNH_2$, EtOH, reflux, 48 h, 90%; (e) 2 M $EtNH_2$, EtOH, reflux, 1 h, 86%; (f) morpholine, EtOH, reflux, 24 h, 87%; (g) thiomorpholine, EtOH, reflux, 48 h, 67%; (h) BCl_3, CH_2Cl_2, 0 °C, 0.5 h, 56–99%.

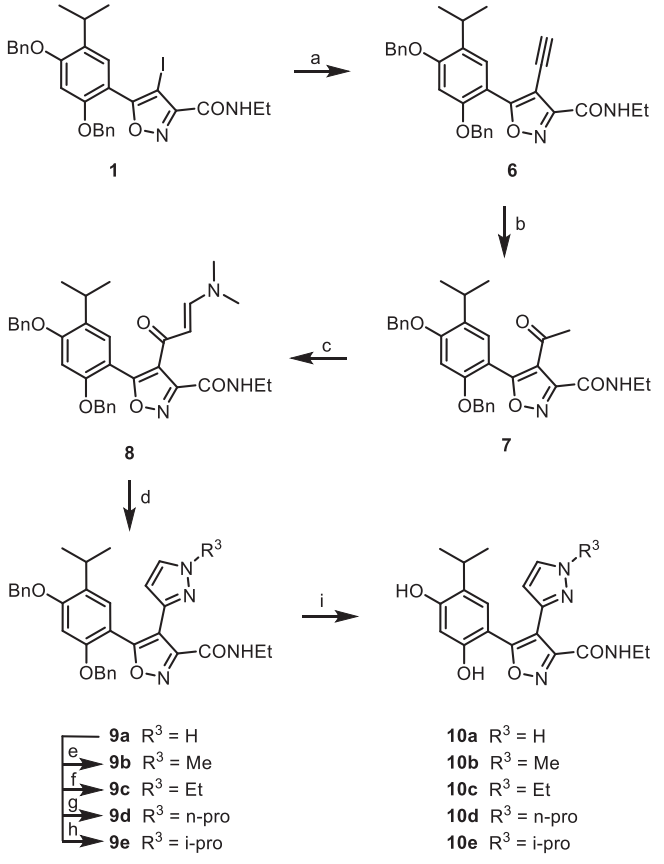

Scheme 3. Synthesis of 3-substituted pyrazole derivatives. *Reagents and conditions*: (a) ethynyltributyltin, $Pd(PPh_3)_4$, toluene, reflux, 2 h, 75%; (b) HCOOH, $NaHCO_3$, 95 °C, 1 h, 45%; (c) *N*,*N*-dimethylformamide dimethylacetal, EtOH, reflux, 4 h, 76%; (d) NH_2NH_2, EtOH, r.t., 48 h, 99%; (e)-(h) R^3I, K_2CO_3, CH_3CN, 1 h, 78–87%; (i) BCl_3, CH_2Cl_2, 0 °C, 0.5 h, 40–99%.

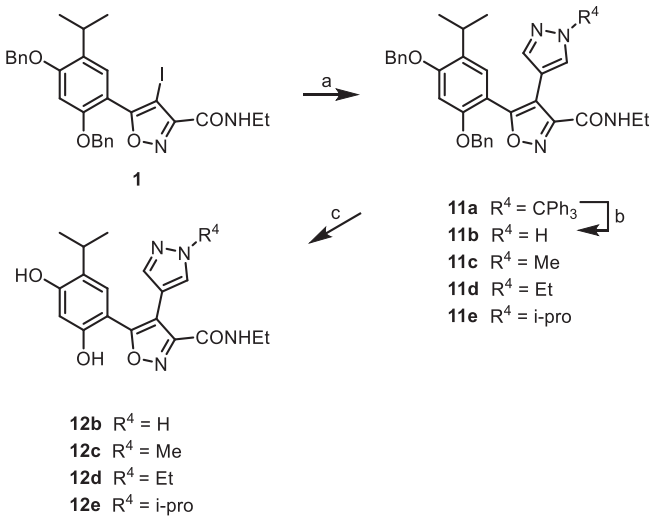

Scheme 4. Synthesis of 4-substituted pyrazole derivatives. *Reagents and conditions*: (a) 4-(tributylstannyl)-1-R^4-1H-pyrazole, $Pd(PPh_3)_4$, toluene, reflux, 12 h, 60–99%; (b) CF_3CO_2H, CH_2Cl_2/MeOH, 75 °C, 3 h, 99%; (c) BCl_3, CH_2Cl_2, 0 °C, 0.5 h, 34–87%.

Table 1
In vitro activity of the isoxaole-CH_2R^1 surrogates.

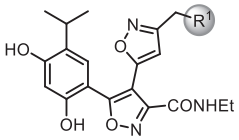

	R^1	IC_{50} (μM)			
		ATPase	Her2	A2780	HCT116
NVP		0.500	0.012	0.006	0.02
4a	OH	0.279	0.042	0.005	0.013
4b	OCH_2CO_2Me	0.443	ND	ND	0.262
4c	OCH_2CO_2H	1.28	ND	ND	ND
4d	OCH_2CONH_2	0.452	0.05	ND	0.097
4e	OMs	0.476	ND	ND	0.4
4f	F	0.41	0.027	0.028	0.063
4g	CN	0.47	ND	ND	0.079
4h	NH_2	0.674	0.171	ND	0.084
4i	NHMe	0.436	ND	ND	0.164
4j	NHEt	0.475	0.023	0.045	0.045
4k	NH-*n*-propyl	0.465	0.024	ND	0.117
4l	NH-isopropyl	0.521	0.018	0.038	0.109
4m	NH-allyl	0.435	0.067	0.043	0.121
4n	NHCOMe	0.5	0.071	ND	0.167
4o	NHCOEt	0.382	0.05	ND	0.078
4p	$NH(CH_2)_2OH$	0.975	ND	ND	0.111
4q	NMe_2	0.49	0.033	0.031	0.092
4r	NEt_2	0.468	0.052	0.078	0.038
4s	*N*(*n*-propyl)$_2$	0.413	0.117	ND	0.183
4t	morphonyl	0.595	0.05	ND	0.028
4u	piperidinyl	0.752	0.062	0.062	0.093
4v	pyrrolidinyl	0.686	0.038	0.055	0.051
4w	*N*-methylpiperazinyl	0.572	ND	ND	0.34
4x	thiomorphonyl	0.44	0.038	0.064	0.067

ND: not determined.

10e). However, the addition of an *n*-propyl group caused reduced activity. Compared to NVP and the corresponding 1,3-pyrazoles, the 1,4-pyrazole analogues showed similar potencies. Unsubstituted pyrazole **12b** proved to be a potent Hsp90 inhibitor.

The eight compounds selected from the *in vitro* study were evaluated for *in vivo* antitumor activity in a mouse A2780 tumor xenograft model.

Table 2
In vitro activity of the isoxaole-COR[2] surrogates.

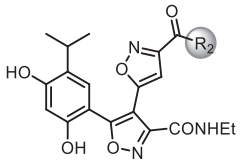

	R_2	IC_{50} (μM)			
		ATPase	Her2	A2780	HCT116
NVP		0.500	0.012	0.006	0.02
5a	OEt	0.447	ND	9	ND
5b	OH	1.87	ND	20	ND
5c	NH_2	0.657	0.052	0.015	0.079
5d	NHMe	0.489	0.024	0.1	0.124
5e	NHEt	0.284	0.028	0.043	0.014
5f	morphonyl	0.583	0.052	0.085	0.060
5g	thiomorphonyl	0.566	ND	0.207	ND

ND: not determined.

Table 3
In vitro activity of the pyrazole surrogates.

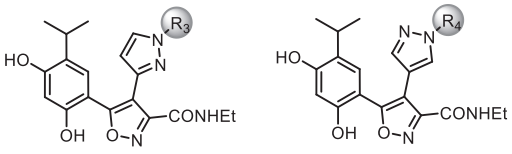

	R_3	R_4	IC_{50} (μM)			
			ATPase	Her2	A2780	HCT116
NVP	–	–	0.500	0.012	0.006	0.02
10a	H	–	0.524	0.045	0.033	0.036
10b	Me	–	0.522	0.016	0.012	0.016
10c	Et	–	0.553	0.012	0.013	0.025
10d	*n*-pro	–	0.584	0.024	0.027	0.049
10e	i-pro	–	0.543	0.014	0.045	0.019
12b	–	H	0.469	0.013	0.038	0.043
12c	–	Me	0.482	0.019	0.02	0.041
12d	–	Et	0.532	0.013	0.03	0.026
12e	–	i-pro	0.542	0.019	0.021	0.021

Table 4
Antitumor activity of selected compounds against human tumor xenograft models (A2780).[a]

	Dose (mg/kg)	route	Frequency	TGI (%)[b]	mortality
NVP	50	i.v.	(3/week) × 3	48.0	0/6
4a	50	i.v.	(3/week) × 3	47.0	0/6
4j	50	i.v.	(3/week) × 2	40.3	0/6
4m	50	i.v.	(3/week) × 2	53.0	0/6
4r	50	i.v.	(3/week) × 2	12.8	0/6
5e	50	i.v.	(3/week) × 3	52.0	0/6
10a	50	i.v.	(3/week) × 2	46.4	0/6
10e	50	i.v.	(3/week) × 2	49.8	0/6
12b	50	i.v.	(3/week) × 2	47.6	0/6

[a] BALB/c-nu/nude mice (n = 6) transplanted with tumor cells were treated with resorcinol compounds.
[b] Tumor growth inhibition: [1-(mean volume of treated tumors)/(mean volume of control tumors)] × 100%.

For the tumor model, A2780 human ovarian adenocarcinoma cells were cultured and implanted into nude mice, and 5 or 6 days later, tumor size and volume were measured. The compounds were suspended in 1% carboxymethyl cellulose (CMC) and were administered intravenously (iv) at a dose of 50 mg/kg three times weekly for two or three weeks. Luminespib (NVP) was used as a reference for comparison.

Table 5
Antitumor activity of selected compounds against human tumor xenograft models (NCI-H1975).[a]

	Dose (mg/kg)	route	Frequency	TGI (%)[b]	mortality
NVP	150	i.v.	(1/week) × 3	43.5	0/6
4a	200	i.v.	(1/week) × 3	50.9	0/6
5e	200	i.v.	(1/week) × 3	44.0	0/6
12b	200	i.v.	(1/week) × 3	55.4	0/6

[a] BALB/c-nu/nude mice (n = 6) transplanted with tumor cells were treated with resorcinol compounds.
[b] Tumor growth inhibition.

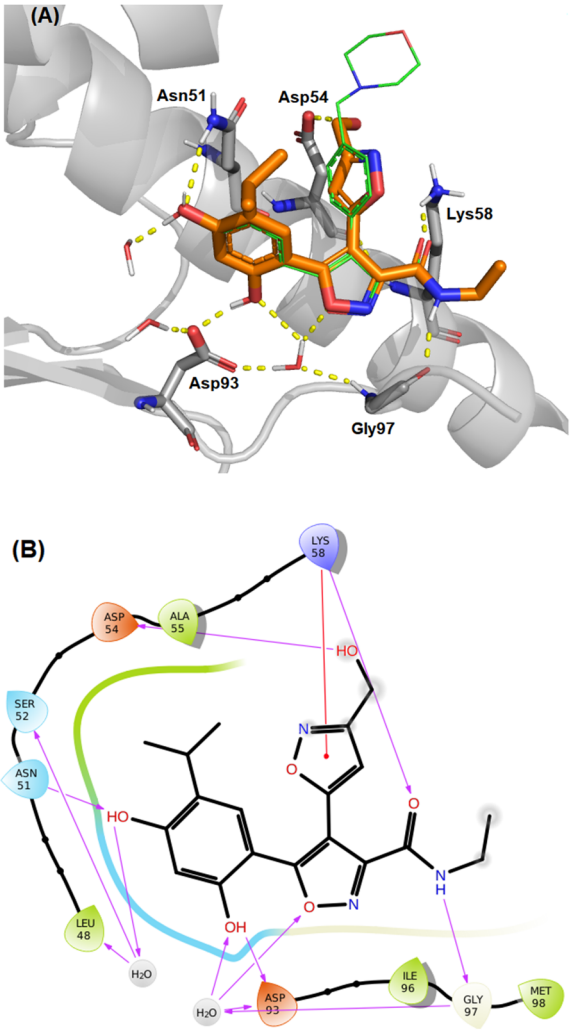

Fig. 2. Predicted binding mode. (A) The binding mode of **4a** (orange) and co-crystal ligand (green) in the ATP-binding site of Hsp90. Hydrogen bonds are shown as yellow dashed lines. (B) Ligand interaction diagram. Hydrogen bonds are depicted by magenta lines, and the corresponding π-cation interaction is depicted by the red line.

As shown in Table 4, all the tested compounds except **4r** significantly inhibited tumor growth with a range of TGI = 40.3–53.0% without any death or body weight loss. In particular, compounds **4m, 5e** and **10e** showed higher inhibitions compared to that of NVP.

A further *in vivo* study was conducted in another tumor model (See Table 5). The three compounds (**4a**, **5e**, **12b**) were administered i.v. at 200 mg/kg once weekly for three weeks to athymic mice bearing NCI-

H1975 human lung carcinoma xenografts. While compound **5e** exhibited comparable activity to NVP, compounds **4a** and **12b** displayed higher antitumor growth inhibition than NVP without any death. This dose schedule was well tolerated, and body weight loss was not observed.

To understand the binding mode of **4a**, we performed a docking study of **4a** with an Hsp90 X-ray crystal structure (2VCI.pdb) using Glide SP.[22] As shown in Figure 2, the binding mode of **4a** was similar to that of luminespib (green), which binds to the Hsp90 ATP binding site. The resorcinol moiety of **4a** was located deep in the pocket and had key hydrogen bonding interactions with Asn51, Asp93 and water molecules. Furthermore, the amide group of **4a** formed hydrogen bonds with Gly97 and Lys58. The isoxazole ring made a π-cation interaction with Lys58, and its hydroxymethyl group showed hydrogen bonding with Asp54, features that are not shown with luminespib.

In summary, the molecular chaperone Hsp90 regulates the stability and activity of oncogenic client proteins that play critical roles in tumor proliferation, survival, and transformation, demonstrating that Hsp90 inhibition is a promising strategy for anticancer chemotherapy. As part of our research program to discover novel Hsp90 inhibitors, we investigated isosteric surrogates of the 4-phenyl group appended to the isoxazole in luminespib in which the 4-substituted phenyl group was modified with 3,5-substituted isoxazole and 1,3 (or 1,4)-substituted pyrazole groups as new scaffolds. Among them, compounds **4a**, **5e** and **12b** exhibited not only potent Hsp90 inhibition in ATPase activity and Her2 degradation assays but also significant antitumor activity in the A2780 and HCT116 cell lines. Animal studies indicated that compounds **4a**, **5e** and **12b** exhibited slightly better or comparable activity than luminespib in A2780 or NCI-H1975 tumor xenograft models. The results indicated that isoxazole and pyrazole surrogates of luminespib potentially possess promising features as drug candidates for anticancer therapy. Further studies in animals will be reported in due course.

Declaration of Competing Interest

The authors declare that they have no known competing financial interests or personal relationships that could have appeared to influence the work reported in this paper.

Acknowledgments

This work was supported by a grant (HA17C0053, 1720340) from the Korea Health Technology R&D Project through the Korea Health Industry Development Institute (KHIDI), funded by the Ministry of Health & Welfare, Republic of Korea.

References

1. Whitesell L, Lindquist SL. *Nat Rev Cancer.* 2005;5:761–772.
2. Maloney A, Workman P. *Expert Opin Biol Ther.* 2002;2:3–24.
3. Kamal A, Boehm MF, Burrows FJ. *Trends Mol Med.* 2004;10:283–290.
4. Chiosis G, Vilenchik M, Kim J, Solit D. *Drug Discov Today.* 2004;9:881–888.
5. Sharp S, Workman P. *Adv Cancer Res.* 2006;95:323–348.
6. Neckers L, Ivy SP. *Curr Opin Oncol.* 2003;15:419–424.
7. Fortugno P, Beltrami E, Plescia J, et al. *Proc Natl Acad Sci USA.* 2003;100:13791–13796.
8. Chakraborty A, Koldobskiy MA, Sixt KM, et al. *Proc Natl Acad Sci USA.* 2008;105:1134–1139.
9. Hanahan D, Weinberg RA. *Cell.* 2000;100:57–70.
10. Workman P. *Cancer Lett.* 2004;206:149–157.
11. Stebbins CE, Russo AA, Schneider C, Rosen N, Hartl FU, Pavletich NP. *Cell.* 1997;89:239–250.
12. Roe SM, Prodromou C, O'Brien R, Ladbury JE, Piper PW, Pearl LH. *J Med Chem.* 1999;42:260–266.
13. Tian ZQ, Liu Y, Zhang D, et al. *Bioorg Med Chem.* 2004;12:5317–5329.
14. Rastelli G, Tian Z-Q, Wang Z, Mylesa D, Liua Y. *Bioorg Med Chem.* 2005;15:5016–5021.
15. Solit DB, Zheng FF, Drobnjak M, et al. *Clin Cancer Res.* 2002;8:986–993.
16. de Candia P, Solit DB, Giri D, et al. *Proc Natl Acad Sci USA.* 2003;100:12337–12342.
17. Solit DB, Chiosis G. *Drug Discov Today.* 2008;13:38–43.
18. Brough PA, Aherne W, Barril X, et al. *J Med Chem.* 2008;51:196–218.
19. Shimamura T, Perera SA, Foley KP, et al. *Clin Cancer Res.* 2012;18:4973–4985.
20. Taldone T, Chiosis G. *Curr Top Med Chem.* 2009;9:1436–1446.
21. Lee JS, Cho YS, Chang MH, Koh HY, Chung BY, Pae AN. *Bioorg Med Chem Lett.* 2003;13:4117–4120.
22. Schrodinger. Available online: http://www.schrodinger.com (accessed on 21 February 2020) The Hsp90 was prepared with Protein Preparation Wizard Workflow provided in the Maestro module of Schrodinger Suite 2019-4. The receptor grid generated a 25 x 25 x 25 Å space region centered at the original ligand of the complex structure. The default values were assigned. The docking of 4a was performed using the standard precision (SP) mode in Glide. The docking model of 4a is displayed using PyMOL version 2.0.4.